Supplemental Information for:

An evaluation of M^{2+} interference correction approaches associated with As and Se in ICP-MS using a multi-day dataset along with ICP-MS/MS / HR-ICP-MS based analysis and hierarchical modeling as a means of assessing bias in fortified drinking waters and single component matrices

Skyler Smith[a,f], Roy W. Martin[b], Nicole Hanks[c], Patricia A. Creed[d], Kasey Kovalcik[e], Robert Wilson[f], Kevin Kubachka[f], Judith A. Brisbin[g], Julio Landero Figueroa[h], and John T. Creed[d,*]

[a] University of Cincinnati/U.S. Environmental Protection Agency (USEPA) Research Trainee, Center for Environmental Solutions and Emergency Response (CESER), Cincinnati, OH 45268, USA

[b] USEPA, Center for Environmental Measurement and Modeling (CEMM), Cincinnati, OH 45268, USA

[c] Student Service Contractor, USEPA, CESER, Cincinnati, OH 45268, USA

[d] USEPA, CESER, Cincinnati, OH 45268, USA

[e] USEPA, Center for Environmental Measurement and Modeling (CEMM), Research Triangle Park, NC 27711, USA

[f] U.S. Food and Drug Administration, Forensic Chemistry Center, Cincinnati, OH 45237, USA

[g] USEPA, Office of Ground Water and Drinking Water, Cincinnati, OH 45268, USA

[h] University of Cincinnati, Department of Chemistry, Cincinnati, OH 45221, USA

*Corresponding author: Dr. John T. Creed, US EPA, 26 W. Martin Luther King Drive, Cincinnati, OH 45268; phone: 513-569-7833; fax: 513-569-7757; email: creed.jack@epa.gov

Figure S1: Across mass range response ratio along with some multi-day interference reduction performance characteristic associated with the Low helium and High helium instrument tunes

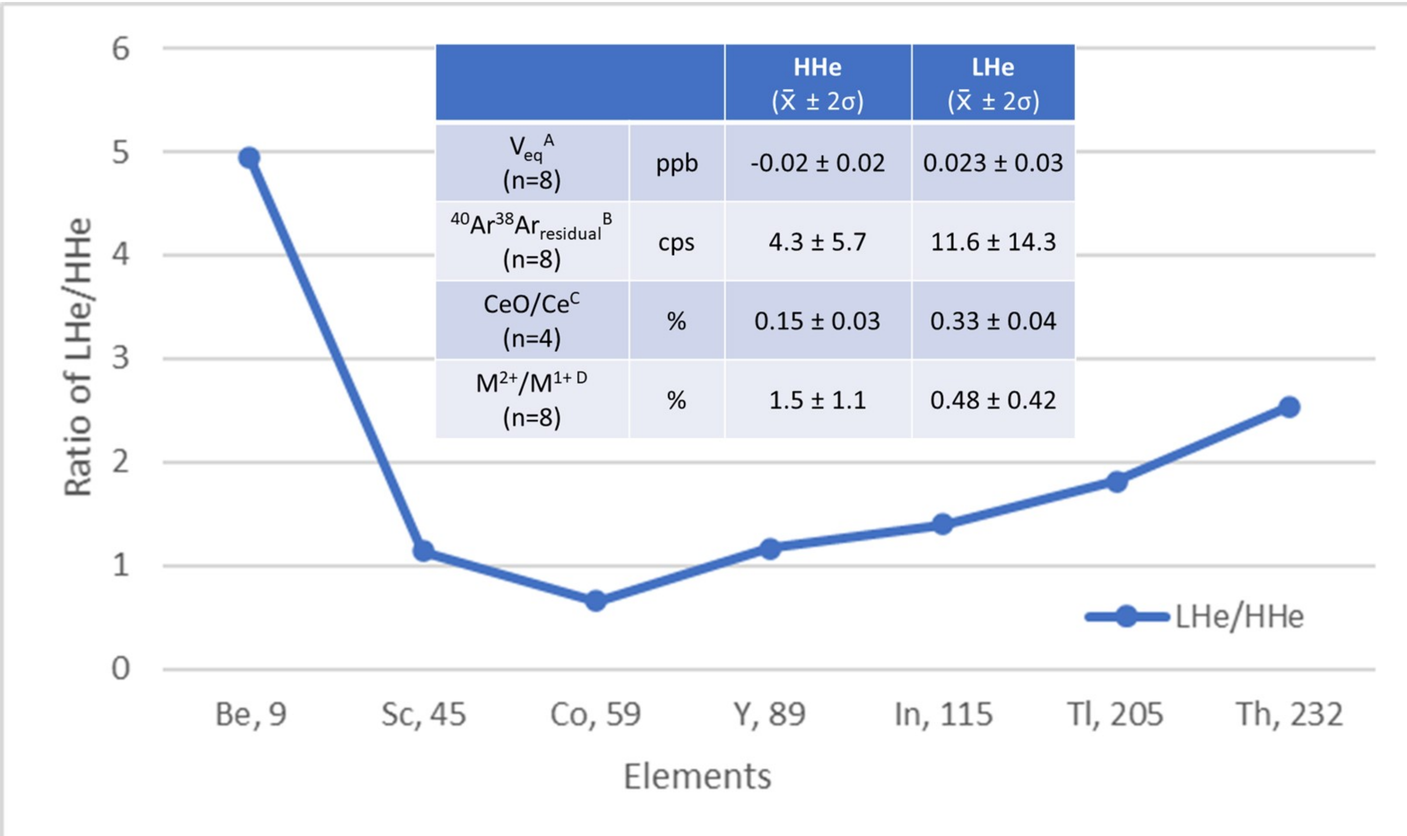

		HHe ($\bar{x} \pm 2\sigma$)	LHe ($\bar{x} \pm 2\sigma$)
V_{eq}[A] (n=8)	ppb	-0.02 ± 0.02	0.023 ± 0.03
$^{40}Ar^{38}Ar_{residual}$[B] (n=8)	cps	4.3 ± 5.7	11.6 ± 14.3
CeO/Ce[C] (n=4)	%	0.15 ± 0.03	0.33 ± 0.04
M^{2+}/M^{1+}[D] (n=8)	%	1.5 ± 1.1	0.48 ± 0.42

A. V_{eq} is the vanadium equivalent concentration reported in a 0.5% HCl solution while the mean and standard deviation are calculated across the eight analysis days
B. $^{40}Ar^{38}Ar_{residual}$ = m/z 78cps in blank – m/z77.5cps in blank. The mean and standard deviation are calculated across the eight analysis days and the cps at m/z 155 in the blanks was less than 381cps for both tunes across all eight days.
C. CeO/Ce is the percent cerium oxide determined using a 10ppb Ce standard while the mean and standard deviation are calculated across four analysis days
D. M^{2+}/M^{1+} is the $^{71.5}Nd^{2+}/^{143}Nd^{1+}$ ratio in the M^{2+} analyte standard while the mean and standard deviation are calculated across the eight analysis days.

Figure S1 and associated table provide a relative response across the mass range along with some collision cell performance measures for the two instrument tunes (LHe, HHe) utilized in this manuscript. Two metrics influence the M^{2+} factor. The first, $^{40}Ar^{38}Ar_{residual}$, estimates the residual argon dimer at m/z 78 across analysis days that could influence a unit mass based M^{2+} factor estimate using ^{156}Gd. The other metric that influences the M^{2+} correction approaches is the magnitude and variability of the M^{2+}/M^{1+} ratio across days for a specific instrument tune. In the table the across day variability of the M^{2+} factor is reported for both the LHe and HHe tune using Nd (71.5/143).

Figure S2: Estimating the $^{150}Nd^{2+}$ false positive on m/z 75 in a sample by applying a dual internal standard correction to the 71.5/143 Nd^{2+} correction factor[1-3]

	71.5 (CPS)	**75** (CPS)	**89** (CPS)	**143** (CPS)	**165** (CPS)
M^{2+} analyte standard	382	456	24,749	106,197	1,884,817
Sample		525	24,224	106,636	1,963,179

Step 1: Estimating the ½ mass M^{2+} Correction Factor for Nd in a sample

$$M^{2+}\,\text{Factor}_{\text{Sample}} = \left(\frac{\left(\dfrac{\text{CPS at } 71.5_{M2+\,Std}}{\text{CPS at } 89_{M2+\,Std}}\right) \times \text{CPS at } 89_{\text{Sample}}}{\left(\dfrac{\text{CPS at } 143_{M2+\,Std}}{\text{CPS at } 165_{M2+\,Std}}\right) \times \text{CPS at } 165_{\text{Sample}}} \right) = \text{Example} \left(\frac{\left(\dfrac{382}{24{,}749}\right) \times 24{,}224}{\left(\dfrac{106{,}197}{1{,}884{,}817}\right) \times 1{,}963{,}179} \right) = 0.0034$$

Step 2: Removing $^{150}Nd^{2+}$ false positive from m/z 75[4]

$$^{150}Nd^{2+} \text{ on m/z } 75 = M^{2+}\,\text{Factor}_{\text{Sample}} \times \text{Isotopic Ratio}^{5} \text{ for } 150/143 \times \text{CPS at } 143_{\text{Sample}}$$

$$\text{Example: } {}^{150}Nd^{2+} \text{ on m/z } 75 = 0.0034 \times 0.555 \times 106{,}636 = 200.1 \text{ CPS}$$

Step 3: After $^{150}Nd^{2+}$ interference is removed the remaining signal is internal standard corrected and a concentration assigned based on a two point-calibration curve

1. In the example Y and Ho are used as internal standards but other internal standard combinations are also evaluated in this manuscript.
2. In the example, the $^{150}Nd^{2+}$ false positive is corrected using the m/z 71.5 and 143 but this approach could be applied to other isotopes for Nd as well as to other odd mass Rare Earths.
3. Both m/z 71.5 and 143 are estimated using the dual internal standard approach. The bias of this estimate is then compared to direct in-sample determination of 71.5/143 using 0.4 amu resolution.
4. A $^{150}Sm^{2+}$ correction could also be required but only the $^{150}Nd^{2+}$ correction is shown in this example.
5. The 150/143 isotopic ratio is determined in the M^{2+} analyte standard using the tune specific conditions.

The stepwise process of correcting for the M^{+2} false positive on arsenic from $^{150}Nd^{2+}$ is outlined in FigureS2. Counts per second signals are given for the masses involved to assure clarity.

Figure S3A: Variability of M^{2+} ratio for 10 odd mass REE in sample matrices analyzed on four separate days using a high helium instrument tune

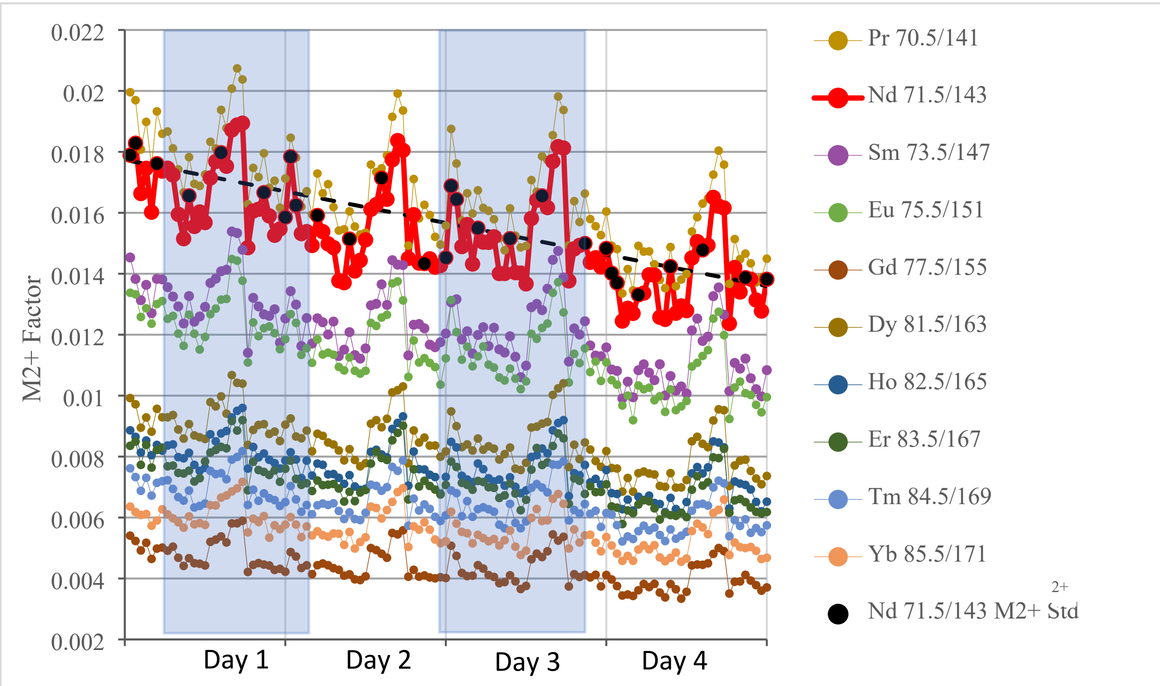

In Figure S3A, the time and matrix dependent shifts in the Nd and Sm M^{2+} factor shown in Figure 1A are extended to include a more complete set of rare earths (Pr-Yb with 0.4amu resolution). The Nd data from Figure 1A have been highlighted in Figure S3A to help visually align the two figures. Both instrument tunes indicate similar profiles but to help with graphical clarity only the data from the HHe tune is presented in Figure S3A. Figure S3A indicates that all the Rare earths (Pr-Yb) exhibit a common time and matrix-oriented variability across all days and this indicates that a M^{2+} correction approach that is applicable for $^{150}Nd^{2+}$ on ^{75}As is likely to be applicable to the $^{156}Gd^{2+}$ correction on ^{78}Se.

Figure S3B: A comparison of in-sample M^{2+}/M^{1+} estimates to dual-internal standard predicted 71.5/143 Nd^{2+} ratios in samples analyzed on four separate analysis days using a high helium flow rate tune [A-C]

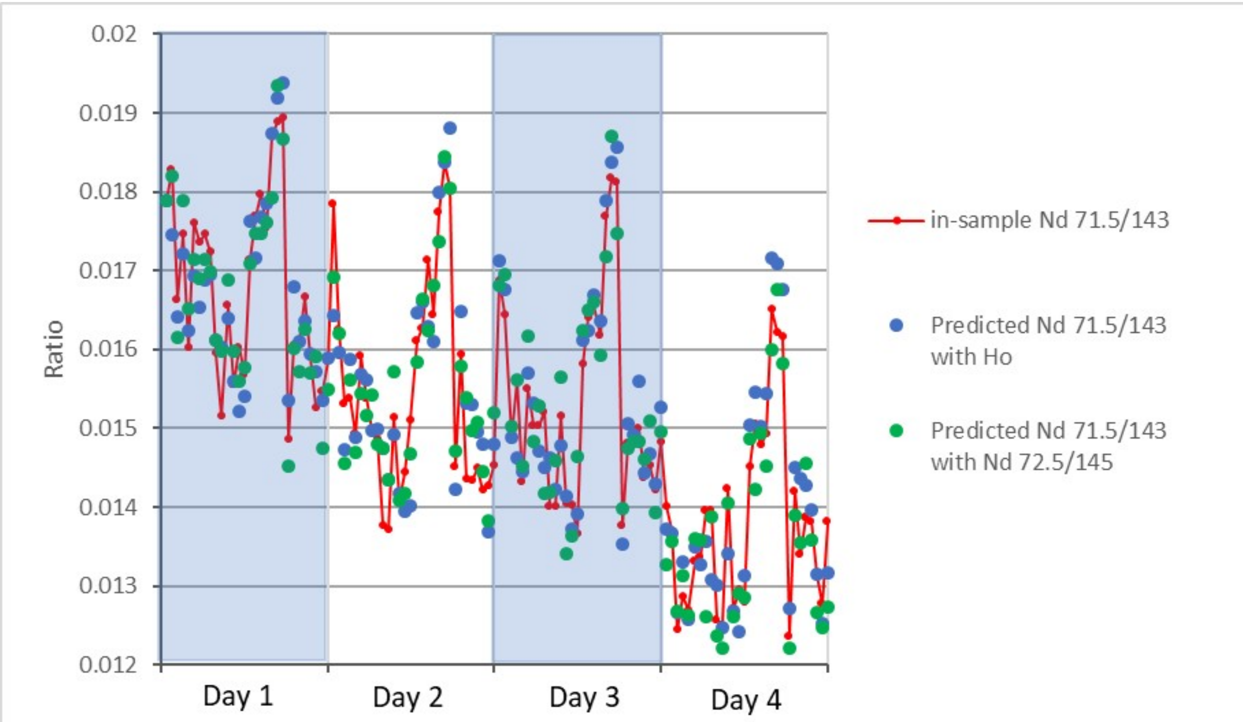

A. Individual sample 71.5/143 Nd^{2+} ratios are predicted using (Ho^{2+}/Ho^{1+}) as a dual internal standard. The predictions are made across sample and day using the first analysis of the M^{2+} analyte standard on the first analysis day
B. Individual sample 71.5/143 Nd^{2+} ratios are predicted using (72.5/145 Nd) as a dual internal standard. The predictions are made across sample and day using the first analysis of the M^{2+} analyte standard on the first analysis day.
C. An average percent recovery and across sample standard deviation were calculated for both the Ho and the alternative isotope-based predictions. The average percent recovery and across sample standard deviation was 102 ± 3.9 for Ho and 98 ± 4.4 for the alternative isotope approach.

In Figure S3B, the ability to predict or estimate the Nd^{2+} ratio across four analysis days based on the first analysis of Nd and Sm containing M^{2+} standard solution on day 1 is evaluated. The two different M^{2+}/M^{1+} dual-internal standard pairs used are: 1.) the alternative odd mass isotope of Nd (72.5/145) as the ideal dual-internal standard pair and 2.) the use of Ho^{2+}/Ho^{1+} as the dual-internal-standard pair (this reflects the approach in Figure 1C) but in this case the impact of matrix is included as an added source of variability. In Figure S3B, the determined 71.5/143 (in-sample, using 0.4amu resolution) ratio are plotted relative to those predicted by the alternative odd mass isotope of Nd and Ho^{2+}/Ho^{1+} internal standard pairs. The predicted estimates are generated by using the 71.5/143 ratio in the first M^{2+} analyte standard on the first day and then applying a dual-internal-standard [Nd, (72.5/145) blue dot or Ho^{2+}/Ho^{1+}, green dot] to predict the M^{2+} ratio across sample and day. This data indicates the potential of a dual-internal-standard approach to correct for M^{2+} false positives in standard solutions and sample matrices.

Figure S4A: A comparison of instrument tune specific across day mean and 95% confidence bounds for selenium (^{78}Se) generated by not applying a M^{2+} correction and by applying a fixed M^{2+} correction factor to samples fortified with 100 ppb Gd.

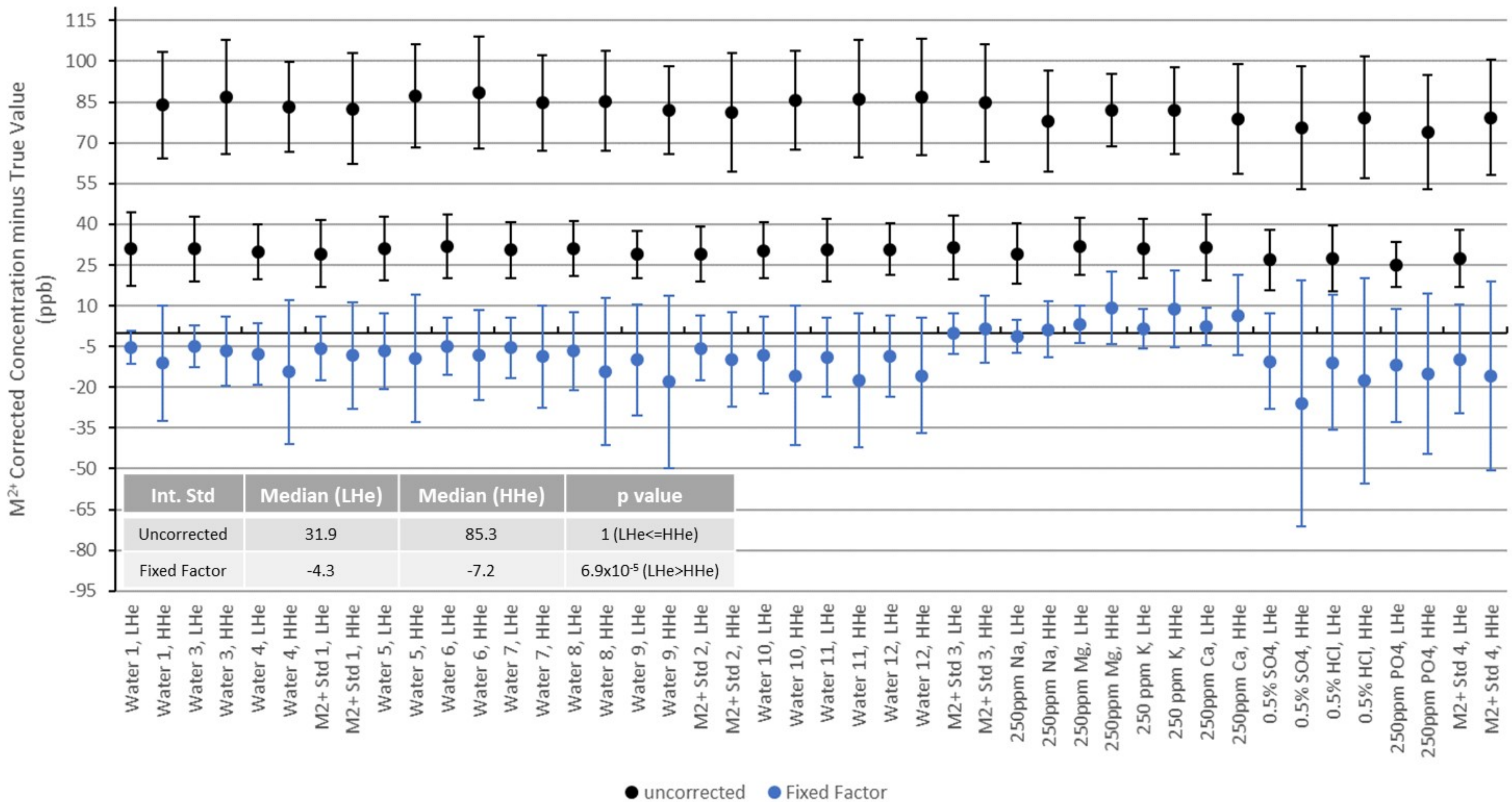

Int. Std	Median (LHe)	Median (HHe)	p value
Uncorrected	31.9	85.3	1 (LHe<=HHe)
Fixed Factor	-4.3	-7.2	6.9×10^{-5} (LHe>HHe)

Figure S4B: A comparison of instrument tune specific across day mean and 95% confidence bounds for selenium (^{78}Se) generated by correcting the sample specific M^{2+} factor using various M^{1+} internal standards treatments in samples fortified with 100 ppb Gd

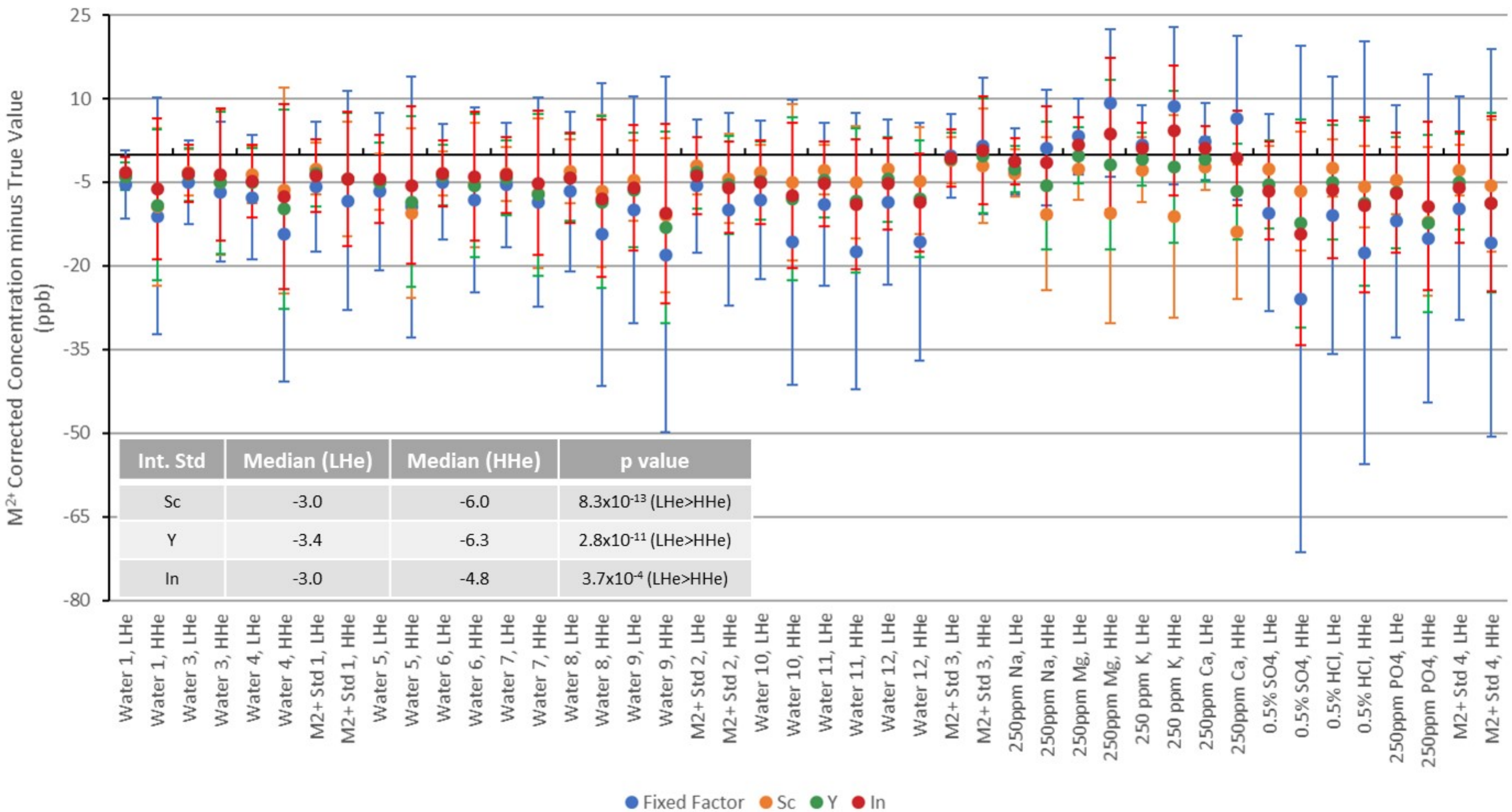

Int. Std	Median (LHe)	Median (HHe)	p value
Sc	-3.0	-6.0	8.3×10^{-13} (LHe>HHe)
Y	-3.4	-6.3	2.8×10^{-11} (LHe>HHe)
In	-3.0	-4.8	3.7×10^{-4} (LHe>HHe)

Figure S4C: A comparison of instrument tune specific across day mean and 95% confidence bounds for selenium (^{78}Se) generated by correcting the sample specific M^{2+} factor using various M^{2+} internal standards treatments in samples fortified with 100 ppb Gd

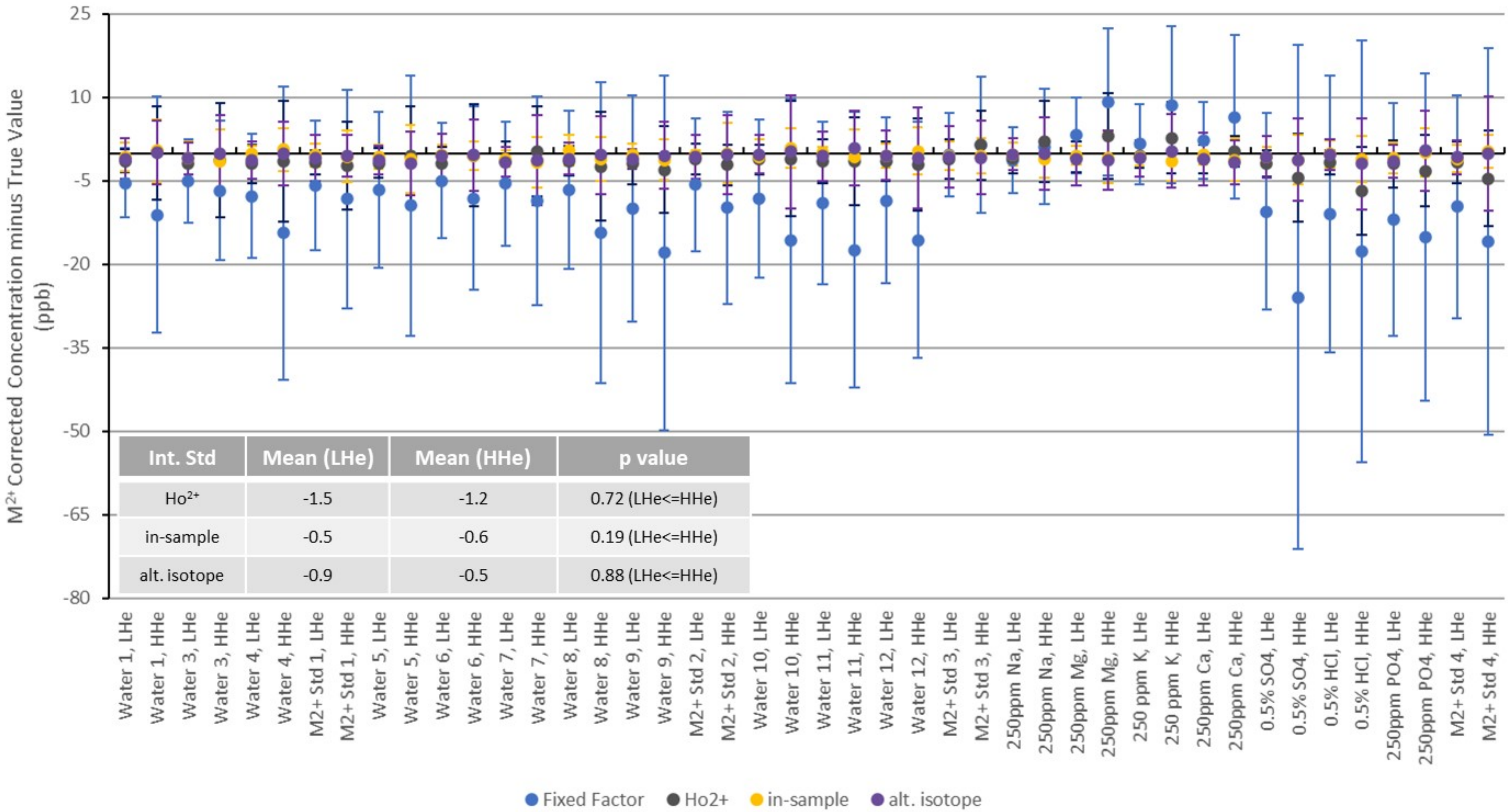

Int. Std	Mean (LHe)	Mean (HHe)	p value
Ho^{2+}	-1.5	-1.2	0.72 (LHe<=HHe)
in-sample	-0.5	-0.6	0.19 (LHe<=HHe)
alt. isotope	-0.9	-0.5	0.88 (LHe<=HHe)

Figure S4A-C provide M^{2+} correction estimates for Se across the eight analysis days utilizing the same internal standard approaches applied to As in Figure 3A-C. The instrument tune specific and 2σ reported in each figure are determined using the analysis conducted on 8 separate days for that specific sample matrix. Similar too Figure 3A-C, the statistical test and associated p-value are performed on individual internal standard treatments with the results pooled across all sample matrices (n=176). A Wilcoxon-Mann-Whitney test is used to compare internal standard treatments that are not normally distributed using a H_O is LHe ≤ HHe. A two-tail t-test is used to compare internal standards treatments that are normally distributed using a H_O is Mean of LHe - Mean of HHe ≤ 0.

In Figure S4A, the uncorrected Se results provide an estimate of the magnitude of the $^{156}Gd^{2+}$ interference for the individual instrument tune (LHe median 31.9ppb: HHe 85.3ppb) using 100ppb Gd. A daily fixed factor is also evaluated in Figure S4A and they indicate an over correction. (LHe median -4.3ppb: HHe -7.2ppb) The data treatment specific statistics are summarized in the inset table within Figure S4A and indicate the LHe tune produces median closer to the zero-line in FigureS4A determined by ICP-MS/MS/HR-ICP-MS relative to the HHe tune.

A series of M^{1+} internal standards (Sc, Y and In) are evaluated in Figure S4B. Similar too Figure 3B, the M^{1+} internal standard generate means with less over correction (closer to the zero-line) for the drinking water matrices but the 250ppm matrices don't reflect this same over corrected trend. Again, the statistical test is conducted by pooling the results across all samples and variability in performance across matrix contributes to the lack of normality within the M^{1+} internal standards. This lack of normality dictates a non-parametric test (Wilcoxon-Mann-Whitney) and it indicates that the LHe tune produces median with less overcorrection for each internal standard treatment.

Finally, the use of M^{2+} as an internal standard in Figure S4C produce the same tightening of the sample specific correction relative to a fixed factor observed in Figure 3C. The M^{2+} internal standard generate normally distributed data across all sample matrices indicating a M^{2+} internal standard can correct for drift across matrices and analysis days generating a normally distributed performance where a M^{1+} like Sc tends to generate a negatively skewed distribution across matrix and day. The p-values in the inset table within Figure S4C indicate that the mean value for the HHe tune are closer to the zero line for Ho^{2+} and alternative isotope while the p-values indicate the LHe tune generates mean values closer to the zero value for in-sample based correction.

Figure S5A: Internal Standard Box Plots and p values associated with the Nd^{2+} and Sm^{2+} correction on As for LHe and HHe Tunes

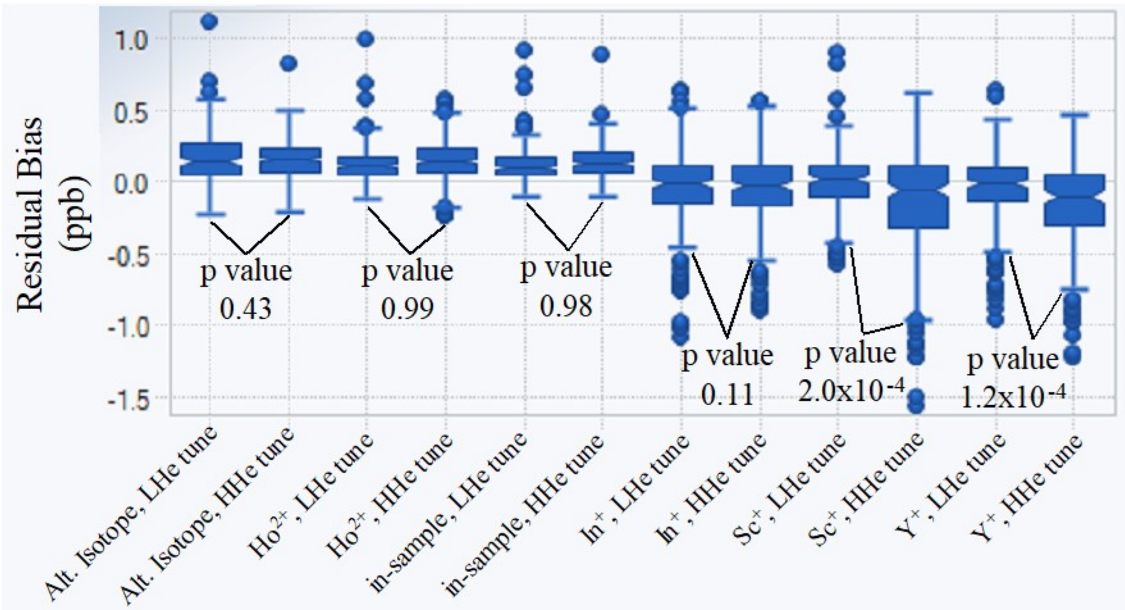

Figure S5A contains a set of box plots for the internal standard and tune specific data associated with the $^{150}Nd^{2+}$ and $^{150}Sm^{2+}$ correction on m/z 75. All the data corrected using a M^{2+} internal standard indicate no statistical difference across the two instrument tunes (LHe, HHe, n=176). The Sc and Y data treatments for LHe and HHe are statistically different while the In treatment was found to not be statistically significant using a $\alpha = 0.05$. The box plots also indicate a slight positive bias (0.1-0.2ppb) for the M^{2+} corrections while the M^{1+} oriented corrections have a slight negative bias. Finally, some of the M^{1+} data treatments indicate a negative skew associated with some of the data entries.

Figure S5B: Internal Standard Box Plots and p values associated with the Gd^{2+} correction on Se for LHe and HHe Tunes

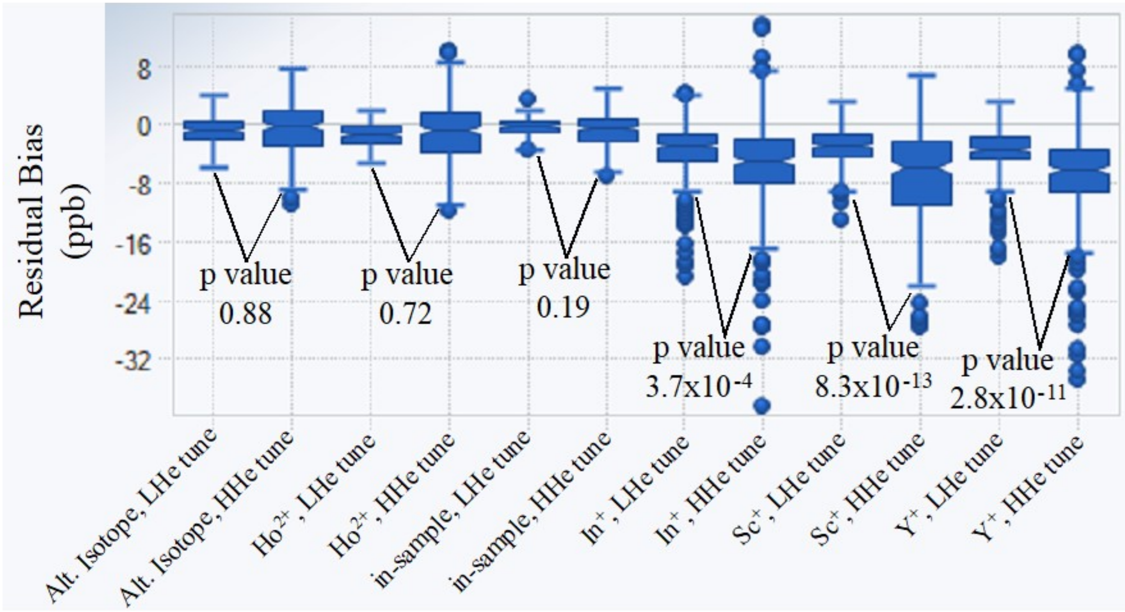

Figure S5B contains a set of box plots for the internal standard and tune specific data associated with the $^{156}Gd^{2+}$ correction on m/z 78. All the data corrected using a M^{2+} internal standard indicate no statistical difference across the two instrument tunes (LHe, HHe, n=176) while all the M^{1+} internal standard treatments were found to be statistically significant using a α= 0.05. The box plots indicate a slight over correction when a M^{1+} oriented corrections are applied. Finally, some of the M^{1+} data treatments indicate a negative skew (over corrections) associated with some of the data entries.

Figure S6A: Matrix-specific predictions of bias from the Bayesian hierarchical model for Se.[1]

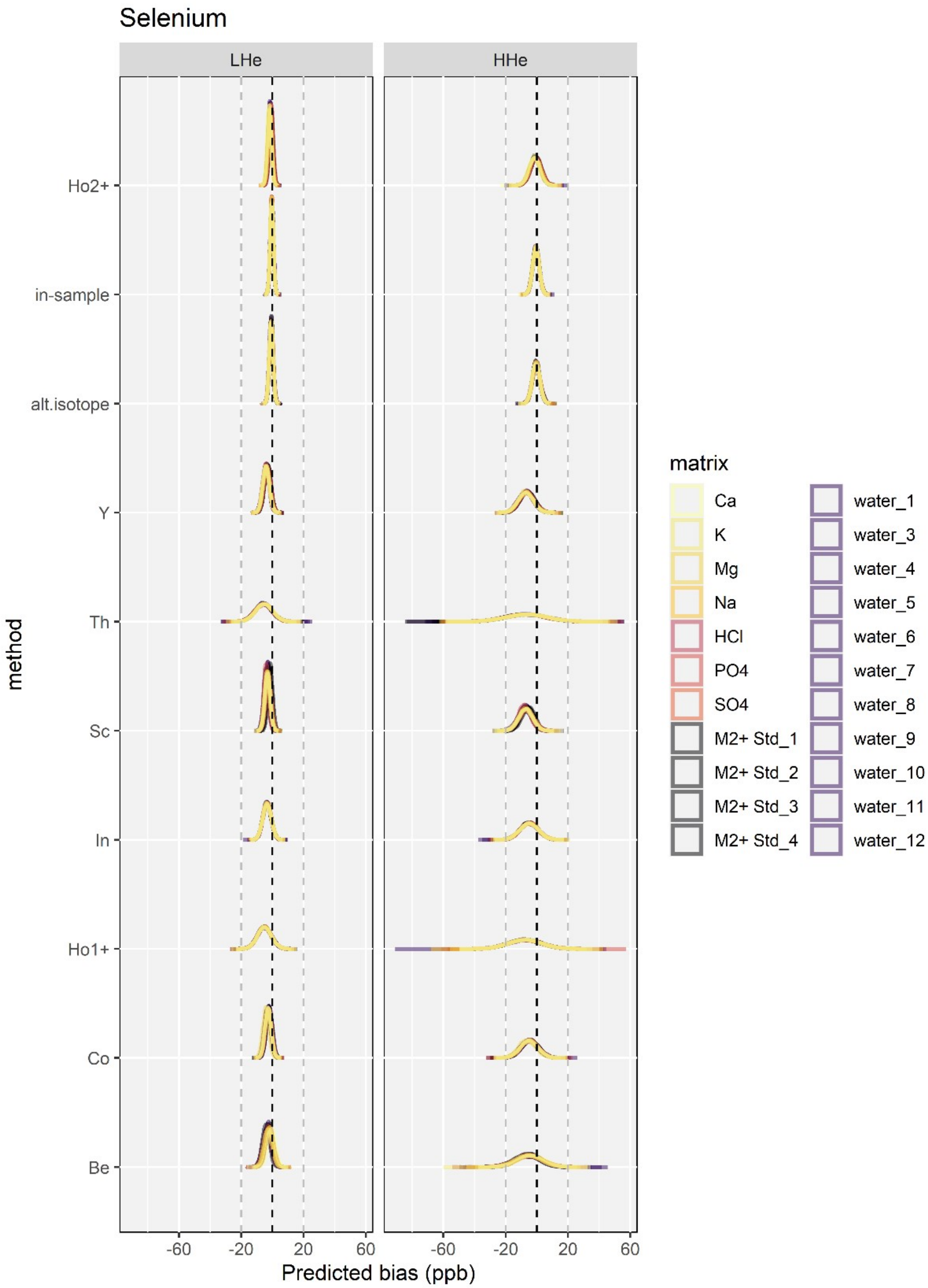

1. Predictions are presented as density estimates based on 6000 draws from the posterior predictive distribution.

Matrix to matrix variation in bias was relatively minimal to negligible across all approaches for Se. This is somewhat of a contrast to the As model inferences regarding matrix, which suggested more influence of the 250ppm matrices on bias, particularly for the M^{1+} internal standard approaches. Likewise, the 250ppm sulfate matrix did not appear to have any outsized effect on the M^{2+} internal standard approaches for Se, as was the apparent case for the M^{2+} internal standard approaches and As. Overall, the M^{1+} internal standard approaches were predicted to consistently over-correct, no matter the matrix. This is in contrast to the As predictions, where most of the M^{1+} internal standard approaches were predicted to be relatively unbiased, on average. Likewise, the in-sample method was predicted to be largely unbiased for Se, whereas it was predicted to under-correct more consistently in the As case. The other M^{2+} internal standard approaches are predicted to slightly over-correct on average for Se, which is also somewhat in contrast to the As predictions, where those approaches were predicted to under-correct, on average. With regard to tune setting, the results for Se were largely in agreement with the results for As: the predictions for the HHe tune are considerably more uncertain (bias more variable) compared to those for the LHe tune. As with arsenic, the tune setting had no clear effect on the mean bias for Se.

Figure S6B: Day-specific predictions of bias from the Bayesian hierarchical model for Se.[1]

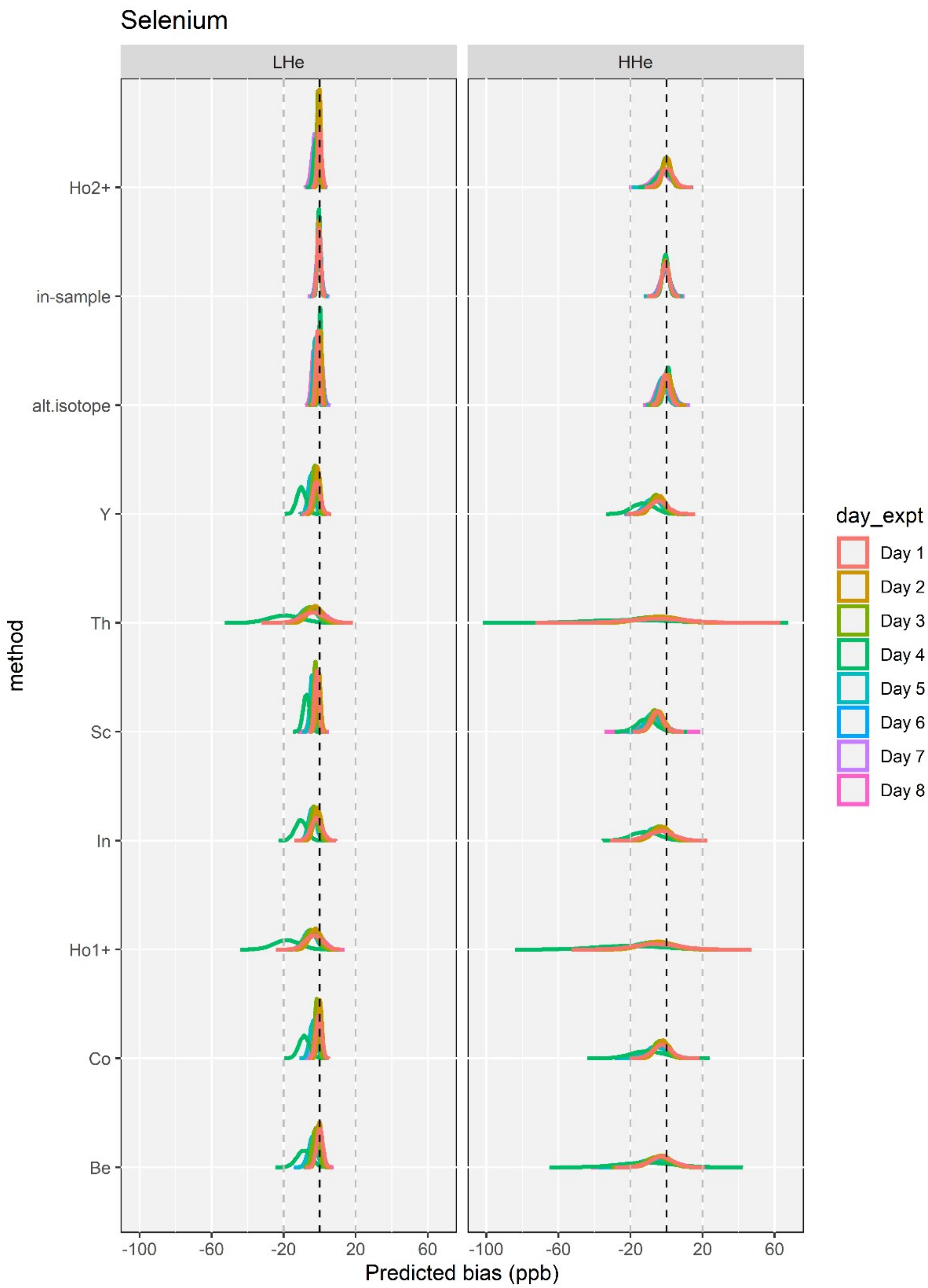

1. Predictions are presented as density estimates based on 6000 draws from the posterior predictive distribution.

Patterns in the predictions of day to day variation in bias for Se were similar to those predicted for As. The extreme over-correction on 3/30 remains for all of the M^{1+} internal standard approaches; and the bias for M^{2+} internal standard approaches was predicted to vary much less across days, by comparison to the M^{1+} internal standard approaches. Overall, the M^{1+} internal standard approaches were predicted to over-correct, on average, for most days, with some exceptions (e.g., Co/Be, Day 1). This is in contrast to the As predictions, where most of the M^{1+} internal standard approaches were predicted to vary more between under- and over-correction across days. Likewise, the in-sample method was predicted to be largely unbiased for Se, on average for all days, whereas it was predicted to under-correct more consistently in the As case. The other M^{2+} internal standard approaches were predicted to slightly over-correct for more days for Se, which is also somewhat in contrast to the As predictions, where those methods were predicted to under-correct, on average, for all days. With regard to tune setting, the results for Se were largely in agreement with the results for As: the predictions for the HHe tune are considerably more uncertain (bias more variable) compared to those for the LHe tune. As with arsenic, the tune setting had no clear effect on the mean bias for Se.

Figure S6C: Predictions of bias from the Bayesian hierarchical model for an average day and matrix[1]

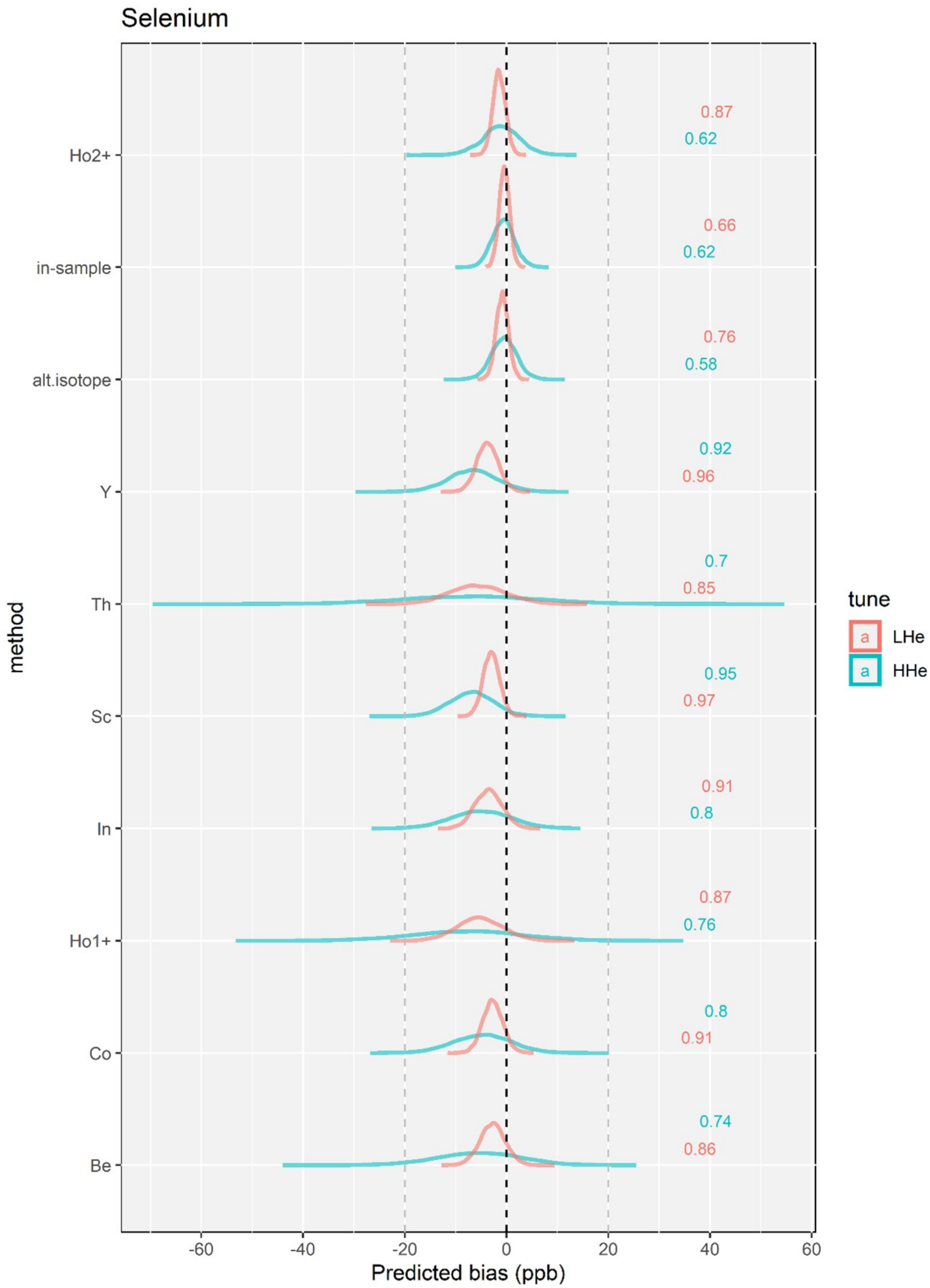

1. Predictions are presented as density estimates based on 6000 draws from the posterior predictive distribution.

In Figure S6C, the model produces estimates for Se corrections for new day assuming an average matrix. The added variability associated with the HHe tune is evident across all internal standard approaches relative to the LHe tune. The M^{2+} internal standard approaches also curtails the variability relative to the M^{1+} oriented approaches. The variability of this plot is larger relative to Figure 4C and this is mainly driven by the differences in the slope of the calibration curve between As and Se. Finally, the probability (proportion of draws < 0 out of 6000) of generating an over corrected (false negative) for each internal standard approach is reported to the right of each internal standard approach.